MICROSTRUCTURAL OBSERVATION AND TENSILE ISOTROPY OF AN AUSTENITIC ODS STEEL

TAE KYU KIM, CHANG SOO BAE[1], DO HYANG KIM[1], JINSUNG JANG*, SUNG HO KIM, CHAN BOCK LEE and DOHEE HAHN
Korea Atomic Energy Research Institute
1045 Daedeokdaero, Yuseong, Daejeon 305-353, Korea
[1]Yonsei University
134 Schinchon, Seodaemun, Seoul 120-749, Korea
*Corresponding author. E-mail : jjang@kaeri.re.kr

Received December 27, 2007
Accepted for Publication April 3, 2008

Based on a composition of 99.4 wt% AISI 316L stainless steel, 0.3 wt% Ti and 0.3 wt% Y_2O_3, an austenitic ODS steel was fabricated by a process of mechanical alloying, hot isostatic pressing and rolling. Fine oxide particles were observed in the matrix, and their chemical formulations were determined to be $Y_2Si_2O_7$ and TiO. Heat treatment of the cold-rolled sample at 1200°C induced an isotropic tensile behavior at room temperature and at 700°C This result would be mainly attributed to the equiaxed grains that form as a result of the heat treatment for recrystallization.

KEYWORDS : Austenitic ODS Steel, Oxide Particles, Tensile Isotopy, Recrystallization Heat Treatment

1. INTRODUCTION

Compared with ferritic-martensitic steels, austenitic steels are known to have superior high-temperature strength and a reliable compatibility with a media, but an inferior irradiation resistance [1,2]. The introduction of an oxide dispersion strengthening concept into these austenitic steels is considered an effective way of improving their irradiation resistance because oxide dispersion strengthened (ODS) steels have been shown to have an excellent irradiation resistance and good high-temperature strength [3-6]. These austenitic ODS steels are thus expected to have an improved irradiation resistance, good high temperature strength, and reliable corrosion resistance, resulting in an attractive candidate material for an in-reactor component such as the cladding tubes of Gen-IV reactors.

For the past two decades, ODS steels have been studied extensively in the nuclear community and considerable progress has been made. For example, ODS steel tubes usually reveal an anisotropic strength in the hoop and longitudinal directions due to a strongly elongated grain morphology [7-10]. One solution to this problem involves a phase transformation for 9-11%Cr ODS steels [7,8] and recrystallization heat treatments for 12-20%Cr ODS steels [9,10]. This solution can effectively modify the strength anisotropy of ODS steels. As a result, ODS steels are recognized as a prospective cladding material for a sodium-cooled fast reactor [6]. However, most of the research on this problem has focused on ferritic-martensitic ODS steels, and the feasibility of austenitic ODS steels has only been studied in a limited way. The fabrication of austenitic ODS steel with isotropic tensile characteristics must therefore be studied. Hence, this study focuses on the microstructure and tensile isotropy of austenitic ODS steel sheets.

2. EXPERIMENTAL PROCEDURE

AISI 316L stainless steel powders were mechanically alloyed (MA) with 0.3 wt% Ti and 0.3 wt% Y_2O_3 powders in a planetary-type ball mill at 200 rpm for 12 hours. The MA powders were placed in an AISI 304L stainless steel container, sealed after a degassing process, and consolidated by a hot isostatic pressing process at 1150°C under a pressure of 103 MPa. A hot isostatic pressed billet was hot-rolled at 1150°C into a plate with a thickness of 4 mm, and then subjected to a subsequent heat treatment at 1150°C for 1 hour. The cold rolling was performed twice with a reduction ratio of about 50% each stage to fabricate a cold rolled sample with a thickness of 1 mm. The intermediate heat treatment was conducted at 1150°C for 1 hour after the first stage of the cold rolling. A cold-rolled sample was heat-treated at 1200°C for 1 hour.

The morphology of the powders was observed by using a scanning electron microscope (SEM). The microstructures were observed by using a transmission electron microscope (TEM), and the elemental analyses of the particles were made by using an energy dispersive spectroscope (EDS) attached to a TEM. The TEM samples were ground to a thickness of 80 μm and then a twin-jet polisher was used at -25°C to electrolytically polish the samples with a mixed solution of 95 vol.% ethanol and 5 vol.% perchloric acid. The optical microstructures were observed by using an optical microscope. The optical microscope samples were prepared by means of mechanical polishing and etching with a mixed solution of 50 vol. % hydrochloric acid, 30 vol.% glycerol and 20 vol.% nitric acid. The tensile test specimens with a gage length of 8 mm were prepared in the longitudinal and transverse directions of the steel sheet, and tensile tests were carried out at a strain rate of 6×10^{-3}/s at room temperature and at 700°C in an air atmosphere. The fractured surfaces were observed by using a SEM.

3. RESULTS AND DISCUSSION

Fig. 1 shows AISI 316L stainless steel, Ti, Y_2O_3 and MA powders. The mean particle sizes of the AISI 316L stainless steel and Ti powders are 20 μm and 3 μm, respectively. The Y_2O_3 powders consist of small crystallites with a mean particle size of about 30 nm. The MA powders closely resemble a disk-type lump with an average diameter of about 250 μm and the particles have a very uniform distribution of size. The MA conditions are known to have the capability of controlling the particle size of the MA powders, and the large particles of MA powders are effective in decreasing the oxygen concentration due to their reduced surface area [11,12].

The chemical composition of the austenitic ODS steel is given in Table 1. The concentration of excess oxygen (Ex.O), which is estimated as the total oxygen concentration minus the oxygen concentration in Y_2O_3, was analyzed to be 0.16 wt%. This value refers to the amount of oxygen picked up during the powder metallurgy process. The excess oxygen dissolves in the matrix until it reaches the solubility of the austenitic matrix. The excess oxygen over than the solubility of the matrix may precipitate to form oxide particles in the matrix. Hence, the amount of excess oxygen is considered important in determining the size of oxide particles in ODS alloys.

Fig. 2 shows a bright field TEM image of the hot-rolled and heat-treated austenitic ODS steel. Dispersed particles smaller than 400 nm in diameter were observed in the matrix. The precipitation of particles is thought to

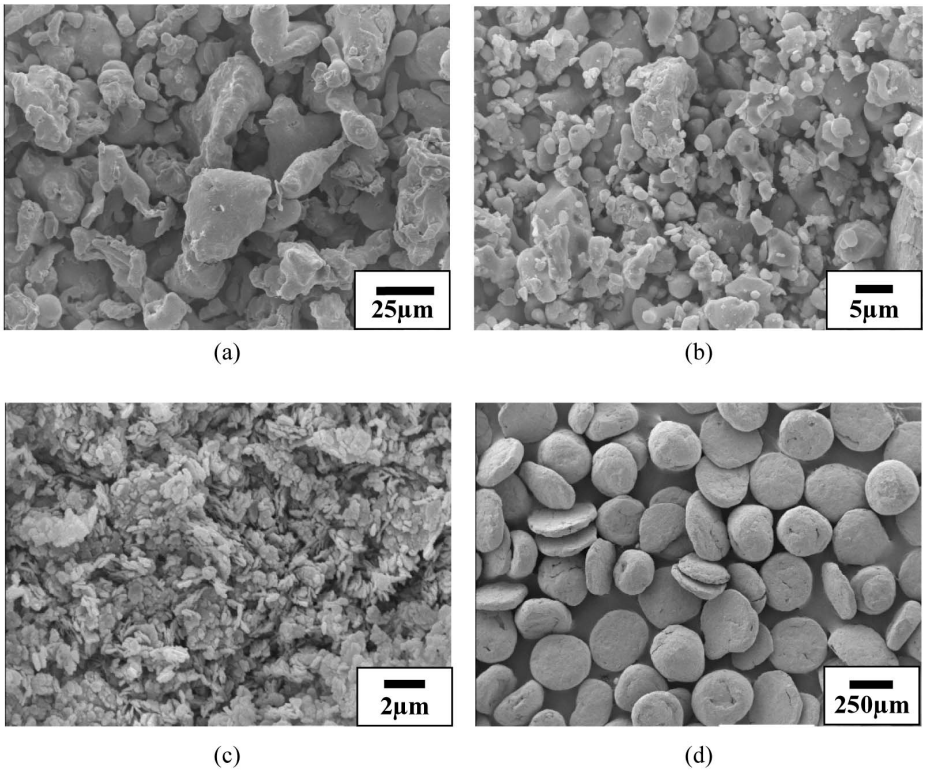

(a) (b)

(c) (d)

Fig. 1. SEM Images of (a) AISI 316L Stainless Steel, (b) Ti, (c) Y_2O_3 and (d) MA Powders Composed of 99.4 wt% AISI 316L Stainless Steel, 0.3 wt% Ti and 0.3 wt% Y_2O_3

Table 1. Chemical Composition of the Austenitic ODS Steel (wt%)

Fe	Cr	Ni	Mo	Mn	Si	C	Ti	Y_2O_3	Ex. O*
Bal.	16.56	11.23	2.19	0.12	0.81	0.029	0.30	0.30	0.16

* Ex. O denotes the excess oxygen, which is estimated as the total oxygen concentration minus the oxygen concentration in Y_2O_3

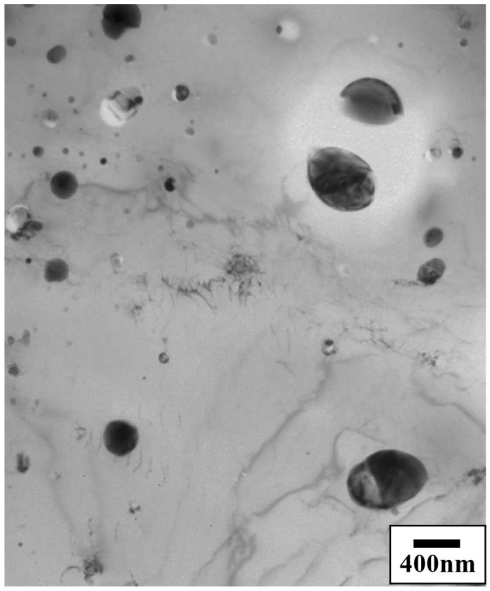

Fig. 2. A Bright Field TEM Image of the Hot-Rolled and Heat-Treated Austenitic ODS Steel

occur during the hot consolidation processes of the hot isostatic pressing and the hot rolling because yttria dissociates and dissolves into the matrix during these processes.

Fig. 3 shows the results of the TEM/EDS observation for the precipitates of the austenitic ODS steel. Two kinds of precipitates with chemical formulations of $Y_2Si_2O_7$ (monoclinic, a = 0.5579 nm, b = 1.0850 nm, c = 0.4696 nm, ß = 95.99°) and TiO (hcp, a = 0.4996 nm, c = 0.2879 nm) were observed. The underlying detailed mechanism of the formation of these precipitates is not obvious and deserves to be investigated. However, the precipitation reactions are assumed to occur in accordance with the following equations:

$$Y_2O_3 + 2Si + 4O\ (Ex.O) = Y_2Si_2O_7 \quad (1)$$

$$Ti + O\ (Ex.\ O) = TiO. \quad (2)$$

The thermodynamic data for $Y_2Si_2O_7$ and TiO need to

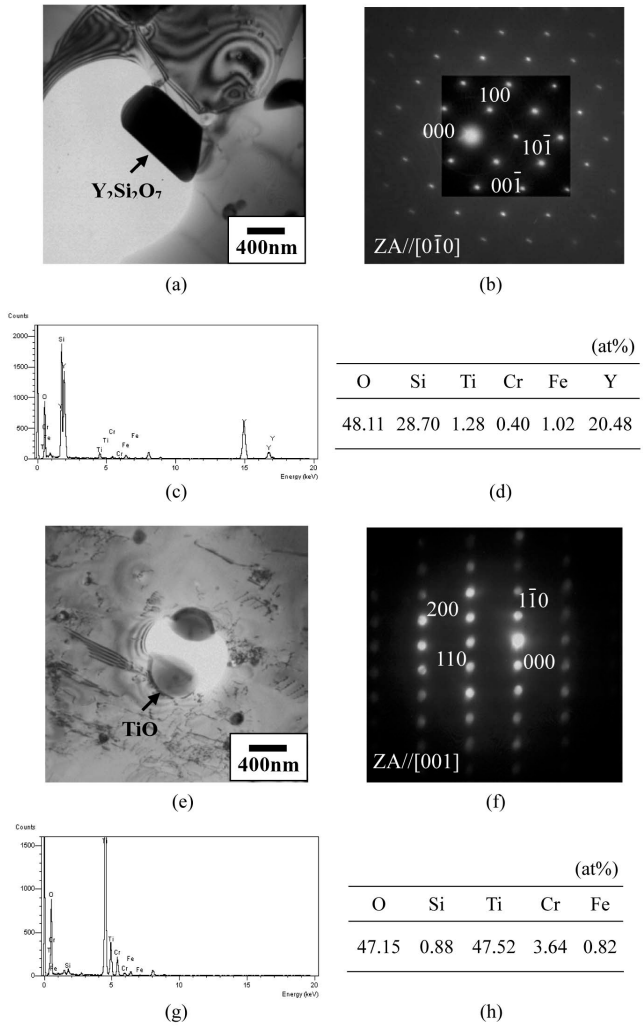

Fig. 3. TEM/EDS Results for the Precipitates of the Austenitic ODS Alloy: (a) Bright Field Image ($Y_2Si_2O_7$), (b) Selected Area Diffraction Pattern, (c) Spectrum, (d) Chemical Composition from the Precipitation Marked by an Arrow in (a), (e) Bright Field Image (TiO), (f) Selected Area Diffraction Pattern, (g) Spectrum, and (h) Chemical Composition from the Prcipitation Marked by an Arrow in (e)

be evaluated if (1) and (2) are thermodynamically favorable. On the basis of the thermodynamic data for $Y_2Si_2O_7$ [13] and TiO [14], the calculated Gibbs free energy change (ΔG) is plotted in Fig. 4 as a function of

temperature. The values of ΔG for (1) and (2) are calculated to be minus, which implies that the formation processes of $Y_2Si_2O_7$ and TiO are thermodynamically favorable. In addition, these ΔG values decrease linearly as the temperature increases.

Fig. 5 shows the optical microstructures for the longitudinal planes of the cold-rolled and recrystallization heat-treated austenitic ODS steels. The grain morphology of the cold-rolled sample appears to be extremely elongated and parallel to the rolling direction; and these characteristics usually cause the tensile anisotropy of the ODS steels. After the final heat treatment, the sample reveals a recrystallized structure. Fig. 6 shows the TEM microstructures of these samples. A high density of dislocations that formed during the previous cold-rolling process was observed in the cold-rolled sample. After heat treatment, most dislocations

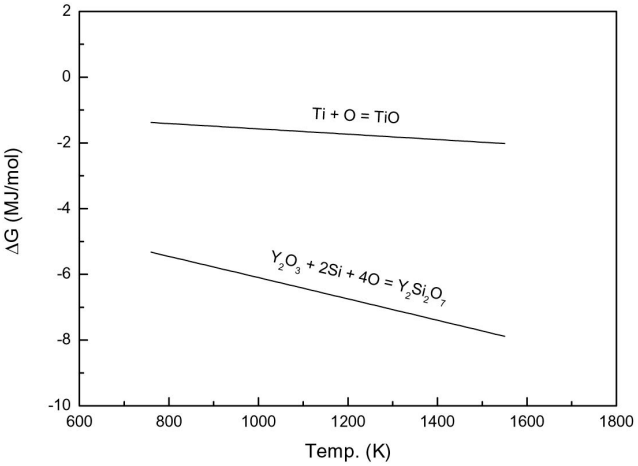

Fig. 4. Gibbs Free Energy Changes for the Precipitation Reactions in the Austenitic ODS Steel as a Function of the Temperature

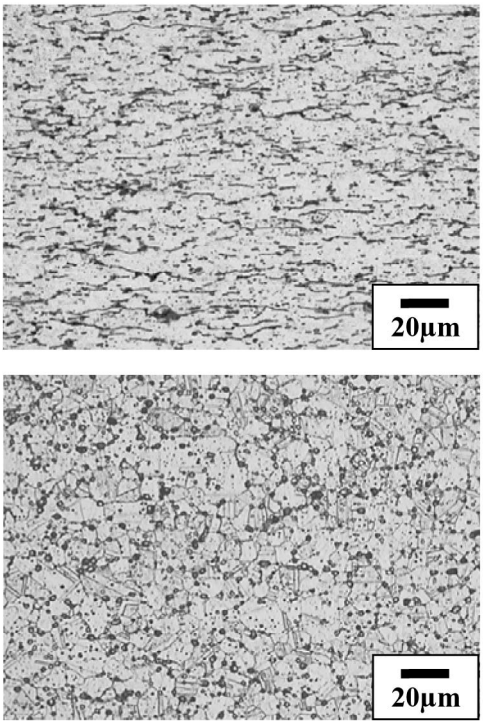

Fig. 5. Optical Microstructures for the Longitudinal Planes of the Austenitic ODS Steel Sheets: (a) Cold-Rolled and (b) Recrystallization Heat-Treated at 1200°C for 1 Hour

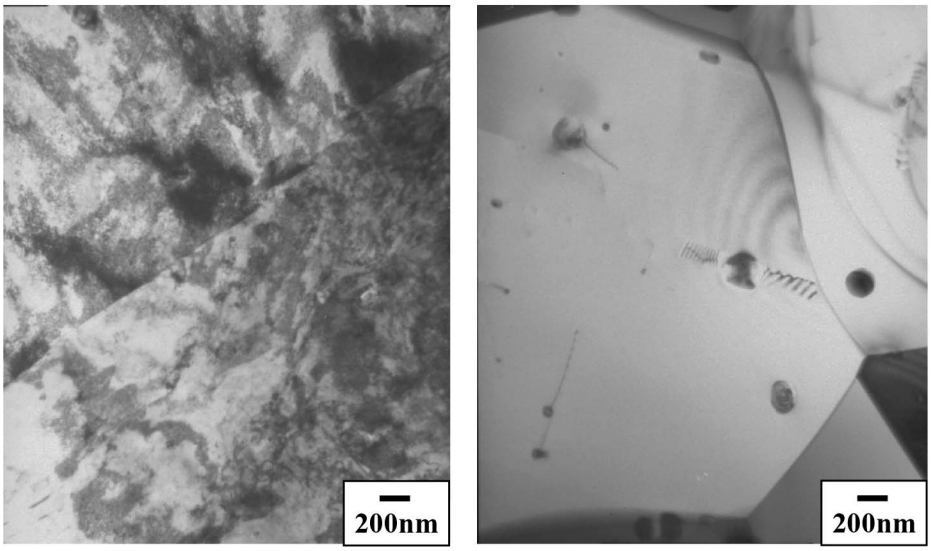

(a) (b)

Fig. 6. A Bright Field TEM Images of the Austenitic ODS Steels: (a) Cold-Rolled and (b) Recrystallization Heat-Treated at 1200°C for 1 Hour

disappear and a fully recrystallized and equiaxed grain structure with an average grain size of about 3 μm can be observed.

Fig. 7 shows the tensile test results for the longitudinal and transverse directions of the recrystallization heat-treated austenitic ODS steel at room temperature and at 700°C The yield and tensile strengths appear to be

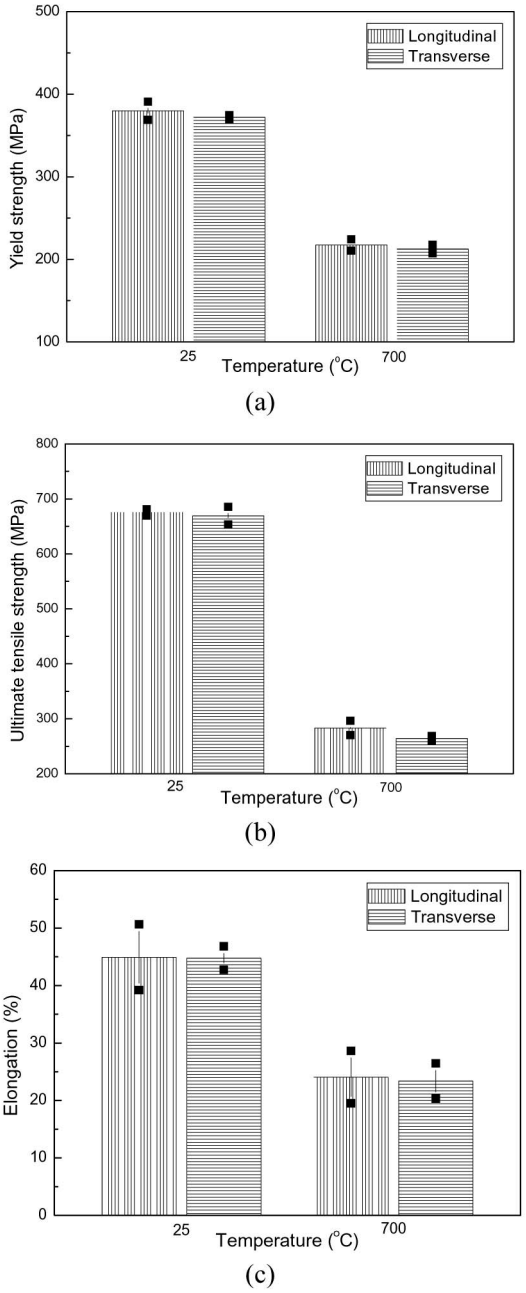

Fig. 7. Tensile Test Results for the Longitudinal and Transverse Directions of the Recrystallization Heat-Treated Austenitic ODS Steels at Room Temperature and at 700°C

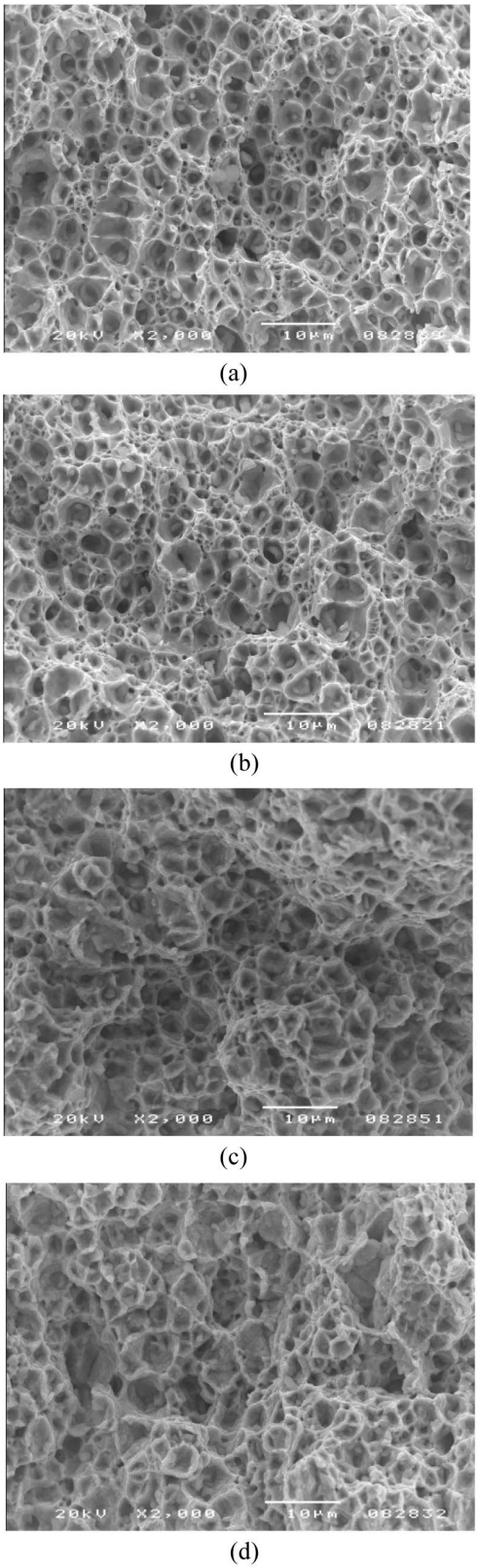

Fig. 8. Fractured Surfaces of the Austenitic ODS Steels after the Tensile Tests: (a) Longitudinal and (b) Transverse Directions at Room Temperature, (c) Longitudinal and (d) Transverse Directions at 700°C

similar in both the longitudinal and transverse directions for the two test temperatures. The elongation is similar in both directions. Thus, the isotropic characteristic of the tensile behavior is mainly attributed to the equiaxed grains during the recrystallization heat treatment (Fig. 6(b)). In addition, the tensile properties of the austenitic ODS steel, which is based on AISI 316L stainless steel, appear to be far superior to those of AISI 316L stainless steel; note that the yield strength, tensile strength, and elongation of AISI 316L stainless steel at room temperature are 176 MPa, 481 MPa and 35%, respectively. These results are mainly attributed to the uniformly distributed oxide particles in the matrix, which can apply high threshold stress to the dislocation motion. The fracture surfaces of the austenitic ODS steels after the tensile tests at room temperature and at 700°C are shown in Fig. 8. The fracture surfaces of all the samples are composed entirely of dimples, and no distinguishable difference can be observed in the fracture surface between the longitudinal and transverse directions. This observation also confirms that the equiaxed grains obtained by the recrystallization heat treatment are effective for an isotropic tensile characteristic.

4. CONCLUSION

An austenitic ODS steel composed of 99.4 wt% AISI 316L stainless steel, 0.3 wt% Ti and 0.3 wt% Y_2O_3 was fabricated by a process of mechanical alloying, hot isostatic pressing, and rolling. Dispersed oxide particles with chemical formulations of $Y_2Si_2O_7$ and TiO were observed, and their formation reactions were thermodynamically demonstrated. The grain morphology control of the cold-rolled sample induced an isotropic characteristic in the tensile strength and ductility at room temperature and at 700°C This characteristic is mainly attributed to the equiaxed grains that form as a result of the heat treatment for recrystallization.

ACKNOWLEDGEMENT

This study was supported by the Korea Science and Engineering Foundation and the Korean Ministry of Education, Science and Technology, through the National Nuclear Technology Program.

REFERENCES

[1] N. Akasaka, S. Yamashita, T. Yoshitake, S. Ukai, A. Kimura, "Microstructural Changes of Neutron Irradiated ODS Ferritic and Martensitic Steels", *J. Nucl. Mater*., **329-333**, 1053 (2004).

[2] R.L. Klueh, and A.T. Lelson, "Ferritic/Martensitic Steels for Next-Generation Reactors", *J. Nucl. Mater*., **371**, 37 (2007).

[3] A. Alamo, V. Lambard, X. Averty, and M.H. Mathon, "Assessment of ODS-14%Cr Ferritic Alloy for High Temperature Applications", *J. Nucl. Mater*., **329-333**, 333 (2004).

[4] T. Yoshitake, Y. Abe, N. Akasaka, S. Ohtsuka, S. Ukai, and A. Kimura, "Ring-Tensile Properties of Irradiated Oxide Dispersion Strengthened Ferritic/Martensitic Steel Claddings", *J. Nucl. Mater*., **329-333**, 342 (2004).

[5] S. Yamashita, N. Akasaka, and S. Ohnuki, "Nano-Oxide Particles Stability of 9-12Cr Grain Morphology Modified ODS Steels under Neutron Irradiation", *J. Nucl. Mater*., **329-333**, 377 (2004).

[6] S. Uki, S. Mizuta, M. Fujiwara, T. Yoshitake, T. Okuda, M. Fujiwara, S. Hagi, and T. Kobayashi, *J. Nucl. Sci. Technol*., **283-287**, 702 (2000).

[7] S. Uki, S. Mizuta, M. Fujiwara, T. Okuda, and T. Kobayashi, "Development of 9Cr-ODS Martensitic Steel Claddings for Fuel Pins by means of Ferritic to Austenitic Rphase Transformation", *J. Nucl. Sci. Technol*., **39**, 778 (2002).

[8] S. Ukai, and M. Fujiwara, "Perspective of ODS Alloys Application in Nuclear Environments", *J. Nucl. Mater*., **307-311**, 749 (2002).

[9] S. Ukai, T. Nishida, T. Okuda, and T. Yoshitake, "R&D of Oxide Dispersion Strengthened Ferritic Martensitic Steels for FBR", *J. Nucl. Mater*., **258-263**, 1745 (1998).

[10] H.Y. Kim, O.Y. Kwon, J. Jang, and S.H. Hong, "Modification of Anisotropic Mechanical Properties in Recrystallized Oxide Dispersion Strengthened Ferritic Alloy", *Scripta Mater*., **54**, 1703 (2006).

[11] H. Sakasegawa, S. Ohtsuka, S. Ukai, H. Tanigawa, M. Jujiwara, H. Ogiwara, and A. Kohyama, "Particle Size Effects in Mechanically Alloyed 9Cr ODS Steel Powder", *J. Nucl. Mater*., **367-370**, 185 (2007).

[12] S. Ohtsuka, S. Ukai, and M. Fujiwara, "Nano-Mesoscopic Structural Control in 9Cr ODS Ferritic/Martensitic Steels", *J. Nucl. Mater*., **351**, 241 (2006).

[13] O. Fabrichnaya, H. J. Seifert, R. Weiland, T. Ludwig, F. Aldinger, and A. Navrotsky, "Phase Equilibria and Thermodynamics in the Y_2O_3-Al_2O_3-$SiO2_2$ System", *Z. Metallkd*., **92**, 1083 (2001).

[14] David R. Lide, *CRC Handbook of Chemistry and Physics*, **72nd ed**., CRC Press, Inc., Boca Raton, Ann Arbor, Boston (1991-1992).